HYDROCHEMICAL VARIATIONS AND CONTAMINANT LOAD IN THE RÍO TINTO (SPAIN) DURING FLOOD EVENTS.

Cánovas, C.R.[(a)] *, Hubbard, C.G.[(b)], Olías, M.[(a)], Nieto, J.M.[(c)], Black, S.[(b)], Coleman, M.L. [(b),(d)]

a) Department of Geodynamics and Palaeontology, University of Huelva, Campus el Carmen, 21071, Huelva, Spain.

b) School of Human and Environmental Sciences, University of Reading, Reading, Berks RG6 6AB, England

c) Department of Geology, University of Huelva, Campus el Carmen, 21007 Huelva, Spain.

d) CALTECH, Jet Propulsion Laboratory, 4800 Oak Grove Dr, Pasadena, CA 91109, USA

* Corresponding Author: Carlos Ruiz Cánovas. Facultad Ciencias Experimentales. Campus el Carmen, s/n, 21007. Tel. +34 959219870 ; Fax. +34 959219440 ; E-mail: carlos.ruiz@dgeo.uhu.es

Abstract

The aim of this work is to study the hydrochemical variations during flood events in the Río Tinto, SW Spain. Three separate rainfall/flood events were monitored in October 2004 following the dry season. In general, concentrations markedly increased following the first event (Fe from 99 to 1130 mg/L; Q_{max} = 0.78 m^3/s) while dissolved loads peaked in the second event (Fe = 7.5 kg/s, Cu = 0.83 kg/s, Zn = 0.82 kg/s; Q_{max} = 77 m^3/s) and discharge in the third event (Q_{max} = 127 m^3/s). This pattern reflects a progressive depletion of metals and sulphate stored in the dry summer as soluble evaporitic salt minerals and concentrated pore fluids, with dilution by freshwater becoming increasingly dominant as the month progressed. Variations in relative concentrations were attributed to oxyhydroxisulphate Fe precipitation, to relative changes in the sources of acid mine drainage (e.g. salt minerals, mine tunnels, spoil heaps etc.) and to differences in the rainfall distributions along the catchment. The contaminant load carried by the

river during October 2004 was enormous, totalling some 770 t of Fe, 420 t of Al, 100 t of Cu, 100 t of Zn and 71 t of Mn. This represents the largest recorded example of this flush-out process in an acid mine drainage setting. Approximately 1000 times more water and 140-8200 times more dissolved elements were carried by the river during October 2004 than during the dry, low-flow conditions of September 2004, highlighting the key role of flood events in the annual pollutant transport budget of semi-arid and arid systems and the need to monitor these events in detail in order to accurately quantify pollutant transport.

Keywords: AMD; Río Tinto; metal load; flood events

1. INTRODUCTION

Acid mine drainage (AMD) is one of the main causes of water pollution worldwide. This water polluting process is mainly related to mining of massive sulphide and coal deposits. Sulphides are stable and very insoluble under reducing conditions, but oxidation takes place when minerals are exposed to atmospheric conditions. Release of acidity, sulphates, iron and accessory metals and metalloids (e.g. Cu, Zn, Co, Cd, Ni, As, etc) from the oxidation of sulphides affects the quality of streams and groundwaters. A detailed description of reactions controlling sulphide oxidation can be found in Nordstrom and Alpers (1999).

The headwaters of the Río Tinto in the SW of Spain (Fig. 1) are situated in the Iberian Pyrite Belt (IPB), which hosts one of the largest concentrations of massive sulphide deposits in the world (Tornos, 2006). The river has attracted a wide range of studies: archaeological investigations (e.g. Nocete et al., 2005) combined with sediment cores from the estuary and continental shelf (Leblanc et al., 2000; Ruiz et al., 1998; van Geen et al., 1997) have shown that the Riotinto mining district has been exploited for at least 4500 years, while the presence of an Fe based ecosystem of extremophile bacteria (González-Toril et al*.,* 2003a; López-Archilla et al*.,* 2001 and 2004) and eukaryotes (Zettler et al., 2002) have garnered interest in the river as a potential natural analogue system for hydrometallurgical processes (González-Toril et al*.,*

2003b, Malki et al., 2006) and extraterrestrial systems (Fernández-Remolar et al., 2003, 2004, 2005).

Amongst the rivers affected by AMD worldwide, Río Tinto is an extreme case of pollution with low pH values (between 1.0 and 3.0) and very high metal and metalloid concentrations along its main course (100 km long). Table 1 shows average concentrations and annual loads of metals and metalloids in several rivers. Río Tinto is extremely polluted, showing values of metal concentration notably larger than the rest of the rivers. Furthermore, in spite of having a drainage basin appreciably smaller, metal loads transported by Río Tinto are in some cases (Cd, and Cu) larger than the metal loads transported by rivers such as Rhone, Elbe and Seine, which drain some of the most industrialised regions in Europe.

The identification of anomalously high trace metal concentrations in the Western Mediterranean Sea and the Gulf of Cadiz (Boyle et al., 1985; van Geen et al., 1991) resulted in a major EU funded project entitled TOROS (Tinto Odiel River Ocean System), which examined the metal biogeochemistry of the Río Tinto and adjacent Río Odiel rivers (Fig. 1), their mixing zones and the Gulf of Cadiz (Achterberg et al., 2003; Braundgardt et al., 2003; Elbaz-Poulichet et al., 2001). The importance of the Tinto and Odiel rivers as metal sources for the Western Mediterranean Sea has led to a number of estimates of the dissolved metal loads transported by these rivers (Braungardt et al., 2003; Olías et al., 2006; Sainz et al., 2004; Sarmiento et al., 2004).

Rivers in mediterranean climate regions, such as Río Tinto, alternate long drought periods with short but intense rainy events during which most of the water discharge, dissolved contaminant, and suspended matter transport occurs. Sainz et al (2004) stated that flood events (discharge > 10 m^3/s) occured on average 17 % of the time but delivered over 50 % of the annual dissolved metal load. Flood events are therefore, key to understanding metal transport processes in this mediterranean catchment. These examples of mass flow are scarcely documented and hence,

largely unknown as previous studies estimating dissolved loads have only sampled the river on a weekly basis (at best) and therefore have failed to accurately capture these key events.

The aims of this work therefore are: 1) to study the hydrogeochemical changes in a highly polluted river such as Río Tinto during storm events; 2) to estimate the mass fluxes that take place during these events, and 3) to quantify the importance of flood events in the annual metal loads into the Ría de Huelva estuary.

2. SITE DESCRIPTION

The source of the Río Tinto is commonly accepted to be in the abandoned mining area of Peña del Hierro (Ferris et al., 2004), some 450 m above sea level. From here the river runs through the Riotinto mining district before flowing down to the Atlantic coast of Spain by the city of Huelva (Fig. 1). The river is approximately 100 km long and drains a catchment with a surface area of 1646 km^2. The Jarrama and Corumbel rivers are its main tributaries (Fig. 1), although they are regulated by reservoirs before their confluences with the Río Tinto.

The upper and middle parts of the catchment are underlain by paleozoic rocks belonging to the Iberian Pyrite Belt (IPB), which comprises of the Phillite-Quartzite (PQ) group overlain by the Volcano-Sedimentary Complex (VSC, formed by slates, shales, volcanic and volcaniclastic rocks) and the Culm group (formed by shales and greywakes). The lower part of the catchment is underlain by Neogene detrital materials (sands, silts, clays, etc.), belonging to the Guadalquivir Basin.

The climate is of a dry mediterranean type with an average rainfall varying between 600 mm in the lower part of the catchment and 1000 mm in the upper northern hills. The rainfall distribution displays great inter- and intra-annual variations, with 70 % of the annual rainfall occurring between October and February, while rainfall is almost non-existent during the dry season from June to September.

The Río Tinto catchment is mainly underlain by low permeability materials and consequently river discharge is highly dependent on the rainfall regime. Olías et al. (2006) showed that during the 1995-2003 period, the Río Tinto's annual average discharge was 50 hm^3, with a mininum value of 6 hm^3 and a maximum of 79 hm^3. River discharge was low (< 1 m^3/s) for 78 % of the recorded days, only exceeding 10 m^3/s in 4% of the days, coinciding with flood events.

The headwaters of the Río Tinto drain the historic mining districts of Peña del Hierro and Riotinto. The Riotinto Mining District is formed by several polymetallic massive sulphide deposits which can be classified in two groups according to their geographical location. Group North is formed by Lago, Dehesa and Salomon deposits, while Group South is constituted by Filon Sur and the big sulphide deposit of San Dionisio. As a consequence of mining activities developed in the area since ancient times, numerous point inputs enter the river from a variety of waste piles associated with mining activities (gangue materials from ore extraction, smelting residues, settling ponds and waste from heap leaching), together with tunnels draining underground workings.

Three main AMD inputs could be differentiated (Hubbard, 2007). At its source, Río Tinto receives leachates from the old mine of Peña de Hierro with a low pH (1.6) and extremely elevated concentrations of sulphate (81 g/L), metal and metalloids (22700 mg/L of Fe, 4600 mg/L of Al, 13 mg/L of As, 27.4 mg/L of Co, etc,) although their most striking characteristic is the low concentration of Cu and Zn (20 mg/L of Cu and 21 mg/L of Zn). Discharges coming from tunnels draining underground workings in the Ríotinto Mining District, such as Tunnel 11 and Tunnel 16 (4.5 and 7.2 km downstream from source, respectively), have higher values of pH (2.7-3.0), Cu and Zn (up to 463 and 528 mg/L, respectively) but lower values of sulphates (up to 18360 mg/L), Fe (up to 3050 mg/L), Al (up to 1330 mg/L), etc. Drainages coming from the Zarandas-Naya mine (8.3 km downstream from the source) join the Rio Tinto waters through the Arroyo Alcojola, which has extremely low pH values (1.2-1.5) and transports large amounts

144 of sulphate (55.5 g/L), metals and metalloids (22100 mg/L of Fe, 1620 mg/L of Al, 538 mg/L of
145 Cu, 540 mg/L of Zn, 99 mg/L of Mn, 88 mg/L of As, etc.).
146
147 The chemical composition of these drainages varies throughout the year owing mainly to
148 hydrologic (i.e. rise of water table, differences in hydraulic behaviour in tailing piles, slag heaps,
149 settling ponds, etc.) biological (bacterial activity) and anthropogenic factors (pumping from mine
150 sites, etc.), recording the highest sulphate and metal concentrations during the summer, when
151 the biotic oxidation processes are more intense, and the lowest during the winter, when dilution
152 by infiltration water takes place.
153
154 The resultant AMD decreases in concentrations and increases in pH as it travels downstream
155 due to dilution from freshwater tributaries (such as the Jarrama and Corumbel rivers) and
156 sorption to/coprecipitation with Fe oxyhydroxides and oxyhydroxysulphates (Galán et al., 2003;
157 Hudson Edwards et al., 1999).
158
159 Despite dilution and sorption/precipitation processes, the river still maintains high concentrations
160 of pollutants before it enters the estuary, with a mean pH of 2.8 (range 2.2-5.0), electrical
161 conductivity of 2.5 mS/cm (range 0.43-9.0 mS/cm) and dissolved metal concentrations of 151
162 mg/L of Fe (range 0.07-2804 mg/L), 18.9 mg/L of Cu (range 0.2-134 mg/L), 26.0 mg/L of Zn
163 (range 2.2-152 mg/L) measured at Niebla, aprox. 61 km downstream of the river source
164 (Cánovas et al., 2007).
165
166 Acidity decreases in the estuary as seawater mixes with riverwater, although metal removal
167 processes are inefficient until high salinities are reached (e.g. Achterberg et al., 2003;
168 Braungardt et al., 2003; Elbaz-Poulichet et al., 1999; López-González et al., 2006). Metal
169 removal processes result in the metallic enrichment of estuarine sediments, with the mobility
170 and bioavailability of metals such as Zn, Cd and Cu being higher in sediments located in the
171 area of fresh water influence than in sediments located in the marine influenced area of the
172 estuary (Nieto et al., 2007).

3. METHODOLOGY

The sampling site was located at a stream-gauge station at Gadea, approximately 41 km downstream of the Riotinto mining area and 50 km downstream of the river's source. Rainfall data have been obtained from pluviometric gauges spread over the catchment (Fig. 1).

Sampling was performed by a Xian 1000 portable autosampler from Bühler Montec. The autosampler consisted of a sample container holding up to 24 bottles and an outlet pipe made of polyethylene. Bottles were washed in 10% (v/v) nitric acid and then with milli-Q water (18.2 MΩ) prior to sampling. Samples were pumped by an air pump vacuum system and manual samples were taken when the autosampler did not work. Before taking a sample, the equipment was automatically purged with river water to avoid sample cross-contamination. The frequency of the sampling was every two, three or six hours depending on the forecast, and being more frequent during flood events (2 hours). Electrical conductivity (EC), pH, redox potential (Eh) and temperature were measured in situ for all samples using portable meters HI-9025C and HI-9033. Samples were filtered through 0.45 μm teflon filters, acidified with suprapure nitric acid to a pH < 2 and refrigerated until analysis.

25 samples were selected for analysis from all those taken in October 2004. Samples were selected when significant changes in pH and EC were observed. The chemical analysis was undertaken at the Central Research Services of the University of Huelva following a custom-designed protocol specific to these types of water (Ruiz et al., 2003). A wide range of major elements (Al, Ca, Cu, Fe, K, Mg, Mn, Na, S, Si and Zn) and trace elements (As, Ba, Be, Cd, Co, Cr, Li, Mo, Ni, P, Pb, Sn and Sr) were analysed using Inductively Coupled Plasma Optical Emission Spectroscopy (ICP-OES) on a Jobin Yvon (JY ULTIMA 2) spectrometer**.** A triplicate analysis was performed in order to evaluate the analytical precision, showing differences below 5% in all cases. Detection limits (3σ of analytical blanks) were below 0.14 mg/L for major elements and 7.04 μg/L for trace elements. The analytical accuracy was checked by the analysis of reference materials (SPS-SW2, TMDA-54.3 and NIST-1640) and an interlab

comparison with the University of Reading (Perkin Elmer Optima 3000 ICP-OES and Elan 6000 ICP-MS), using samples from across the EC range. Most of the elements assessed in the interlab comparison showed differences below 5 %.

Fifteen salt mineral samples were collected in August 2003 and September 2004 and analysed at the University of Reading by XRD with a Bruker D5000 using Diffrac AT software and by XRF with a Philips PW1480 Sequential Spectrometer and (for As) a portable Niton XLt 700 XRF Analyser.

4. RESULTS AND DISCUSSION

4.1 Rainfall and discharge variations

Figure 2 shows the hydrograph during the study period as well as the daily average rainfall recorded in the catchment and the samples analysed for dissolved concentrations. The lack of rainfall during the dry season (June-September) caused the river discharge to decrease from 0.24 m^3/s in June to 0.004 m^3/s at the beginning of October. A comparison of total discharge highlights the extreme seasonality of the Río Tinto with 10.4 hm^3 of water recorded at Gadea in October 2004, compared with a total discharge of 0.01 hm^3 in September. Three different flood events have been identified from the hydrograph.

The river discharge increased from 0.004 to 0.78 m^3/s due to the first rainfall (on the 8^{th} and 9^{th} of October) recorded after a long dry season. This maximum was reached 10 hours after the end of the rainfall. The lag between the rainfall and the hydrograph crest can be explained by the basin concentration time and the low moisture content in the catchment soils after the dry season (Walling and Foster, 1975). After this peak, the discharge decreased gradually to 0.12 m^3/s. Unfortunately, the autosampler did not work during this event so its impact on the river could only be assessed by comparing pre-event and post-event samples from the 2^{nd} and 18^{th} of October.

232

233 The second rainfall event (Event 2) occurred from the 18th to the 21st of October and can be
234 divided into three sub-events with discharge peaks of 0.87 m^3/s (Event 2a), 6.4 m^3/s (Event 2b)
235 and 77 m^3/s (Event 2c). The rising limb of Event 2c was not sampled because sediments
236 mobilised by rapidly rising water levels buried the inlet pipe of the autosampler, although some
237 samples were taken manually during the falling limb. The third and final flood event of October
238 2004 occurred on the 27th as a consequence of an average rainfall in the catchment of around
239 80 mm. This event had the highest peak discharge (127 m^3/s) recorded in the month. The falling
240 limb appeared to be stepped (Fig. 2), which can be explained by the water released into the Río
241 Tinto from the Jarrama reservoir (Fig. 1) on the 28th (2.2 hm^3) and the 29th (1.4 hm^3).
242

243 **4.2 Hydrogeochemical variations**
244

245 In order to analyze the hydrogeochemical changes during storm events that occur after a long
246 dry season in a complex system like Río Tinto, it is necessary to consider all the processes and
247 sources that might affect the water composition: 1) washout of soluble efflorescent salts
248 precipitated during the summer; 2) dilution by runoff freshwater; 3) spatial variations of rainfalls
249 between undisturbed and mining areas; 4) precipitation of iron mineral phases; and 5) variations
250 in contribution from different AMD inputs.
251

252 Basic statistics from samples collected during the storm events are shown in Table 2. Figure 3
253 shows variations in pH, EC and some dissolved compounds throughout the flood events.
254 Sulphate concentrations increased dramatically following Event 1 from 1.6 g/L on 02/10/04 to
255 9.5 g/L on 18/10/04 reaching an apparent steady state of elevated concentrations. This could be
256 caused by the dissolution of soluble evaporitic salt minerals accumulated on the banks of the
257 Río Tinto and on/in spoil heaps in the Source Zone (Buckby et al., 2003; Lottermoser, 2005) or
258 by water richer in sulphate emanating from other AMD sources.
259

During this first event, most elements raised their concentration, being As the element which showed the maximum increase (nearly 2 orders of magnitude). However some elements such as Na, Sr and K underwent a slight decrease.

Concentrations remained high through Event 2a with some elements increasing (e.g. Fe, As and Pb) while others remained constant (e.g. Al, Co, Mn, Ni, Zn), despite the increase in discharge. The slow dissolution of less soluble mineral phases owing to the acidity released by dissolving the evaporitic salt minerals, could explain this increase. Pb and mainly As, have a great affinity to be adsorbed onto Fe mineral phases (e.g Zänker et al., 2002; Acero et al., 2006).

Concentrations then decreased steadily through Event 2b although Pb (Fig. 3), and Ba exhibited a different behaviour. The crest of the hydrograph for Event 2b did not occur at the same time as the minimum value of EC and sulphate and metal concentrations (Fig. 3). Variations in concentration of dissolved elements usually show a lag with water discharge (Lee and Bang, 2000; Sandén et al., 1997; Walling and Foster, 1975), which is inversely related to antecedent catchment soil moisture and rainfall magnitude. No such lag was apparent for Event 3 (Fig. 3) when soils were wetter and rainfall was more intense.

By the end of Event 2c, the flushout of evaporative salts must be complete, resulting in lower concentrations than pre-Event 1 values. Similar trends have been observed in Contrary Creek, Virginia by Dagenhart (1980) and Boulder Creek, Iron Mountain, California by Keith et al. (2001).

During Event 1 pH decreased very slightly from 2.31 to 2.27 (Fig.3), despite the increase in discharge. In comparison, the large influxes of freshwater in Event 2c (Q_{max} = 76.8 m^3/s) and Event 3 (Q_{max} = 127 m^3/s), when soluble salts are washed, increased pH to 3.56 and 3.36 respectively.

289 The mineralogy and chemistry of 15 salt mineral samples collected in August 2003 and
290 September 2004 are summarised in table 3. In addition to iron-rich salt minerals (copiapite,
291 coquimbite, melanterite, rozenite and szomolnokite), XRD identified variable quantities of
292 minerals containing Al (alunogen, aluminocopiapite and halotrichite), Ca (gypsum) and Mg
293 (hexahydrite). Absolute and relative concentrations were highly variable (Table 3). Wide
294 variations in mineralogy and chemistry have been noted before in salt minerals from the Río
295 Tinto (Buckby et al., 2003; Lottermoser, 2005) and other mining regions (e.g. Keith et al., 2001).
296
297 Fe/SO_4 ratios were generally higher during the flood events than during the low-flow conditions
298 of early October (Fig. 4). Efflorescent soluble salts have higher Fe/SO_4 ratios than river water
299 (Fig. 5a), so their dissolution increases the Fe/SO_4 ratio. Variations in Fe/SO_4 ratios throughout
300 the flood events can be explained by a mixing of freshwater with acidic leachates coming from
301 the Riotinto Mining District (Fig.5a). The dissolution of soluble salts might have a higher
302 influence on water chemistry during the first events, decreasing its significance as these soluble
303 salts are progressively washed. Furthermore, the precipitation of Fe oxihydroxisulphates during
304 the flood peaks 2c and 3 (samples with low Fe/SO_4 in Fig. 5a), when pH values were higher,
305 also diminishes the Fe/SO_4 ratio.
306
307 Cu/Zn and Zn/SO_4 ratios are also shown in figure 4. Cu and Zn should not sorb significantly to
308 Fe oxyhydroxides at the low pH of the waters sampled in this study (Smith, 1999). Lee et al.
309 (2002) investigated metal removal in the laboratory by neutralising 3 AMD streamwaters from
310 Tennessee, USA. They showed that the pH at which 50 % of the metals were removed from
311 solution ranged from 4.6-6.1 for Cu and 5.6-7.5 for Zn. It is therefore unlikely that the variations
312 observed in these ratios (Fig. 4) were due to sorption/coprecipitation processes.
313
314 Alpers et al. (1994) showed that melanterite ($FeSO_4.7H_2O$) preferentially removed Cu to Zn from
315 solution meaning that it should have relatively high Cu/Zn ratios. The decrease in Cu/Zn seen in
316 Event 2c (Fig. 4) should therefore, theoretically, not be due to dissolution of melanterite or its
317 dehydration products (rozenite $FeSO_4.4H_2O$ or szomolnokite $FeSO_4.H_2O$). Furthermore, Buckby

et al. (2003) showed that copiapite (rather than melanterite-suite minerals) was the most abundant salt mineral in the Río Tinto.

The similarity of Event 1 Cu/Zn ratios to pre-Event 1 ratios (Fig. 4) suggests that the weighted average of salt mineral compositions dissolved by Event 1 had similar ratios to the weighted average of summer inputs from the mining area. Variations in these ratios throughout the flood events may well reflect changes in the dominant mine drainage sources into the river (Fig.5b) rather than non-conservative behaviour. Figure 5c shows that variations in Zn/SO_4 ratio in most of samples could be explained as a mixing of two end-members: unaffected freshwaters (end-member A represented by the water composition in the Corumbel reservoir) and Río Tinto water during event 2a (end-member B) as representative of maximum contamination level. Samples located away from this mixing line would indicate the influence of different AMD sources.

4.3. Saturation indices

To examine the phases controlling non-conservative behaviour, saturation indices (SIs) were calculated using the modelling program PHREEQC (Parkhurst and Appello, 1999) and the WATEQ4F thermodynamic database (Ball and Nordstrom, 1991). The database was amended with solubility products for plumbojarosite ($Pb_{0.5}Fe_3(SO_4)_2(OH)_6$, $\log K_{sp}$ = -8.14; Chapman et al., 1983) and schwertmannite ($Fe_8O_8(OH)_{4.5}(SO_4)_{1.75}$, $\log K_{sp}$ = 10.5, Yu et al., 1999). Fe speciation was not analysed in the samples taken in October 2004 but modelling results (based on Eh) indicated an Fe(III) content of 81 % prior to the flood events. The percentage of dissolved Fe(III) increased throughout the flush-out processes, reaching almost 99 % of the total iron at the beginning of Event 2.These values agree with Fe speciation measured by Hubbard (2007) (Fe(III) = 81-98 % of total Fe, n = 5). However, Fe(III) percentages gradually decreased as concentrations were diluted, reaching a minimum Fe(III) content of 3 % of total iron (S20) during the third event. Geochemical modelling showed that all the sampled waters were oversaturated with respect to hematite (SI = 8.7-11.2) and goethite (SI = 3.3-4.6) although kinetic factors mean that these phases tend to form paragenetically from other metastable phases rather than

precipitating directly from solution (Bigham et al., 1996; Nordstrom and Alpers, 1999). In terms of the metastable phases, the samples were generally undersaturated with amorphous $Fe(OH)_3$ (SI = -2.5 to -0.9), as would be expected in these low pH waters, and generally oversaturated with respect to schwertmannite (SI = -4.3 to 5.5) and K-jarosite (SI = -1.6-2.9).

The behaviour of Pb in figure 3 could not be explained from the modelling output by equilibrium with a solid phase as all samples were undersaturated with respect to anglesite ($PbSO_4$, SI ≤ -0.50) and (with the exception of sample S1) oversaturated with plumbojarosite (SI = -0.64 to 3.2). It is possible that a detailed examination of the suspended particulate matter carried by flood events may yield an explanation for Pb behaviour. All samples were oversaturated with respect to barite ($BaSO_4$, SI = 0.2-0.8) although Ba concentrations could potentially be explained by equilibrium with a mixed Ba-Sr sulphate phase as celestite ($SrSO_4$) was undersaturated in all samples (SI ≤ -1.3). Alternatively, barite oversaturation could potentially be explained by colloidal barite (< 0.45 µm) in the samples (Naus et al., 2005). However, Ba is not an important contaminant in this system as sampled concentrations (13-104 µg/L) were all below World Health Organisation drinking water quality guidelines (0.7 mg/L; WHO, 2004).

4.4 Pollutant loads

Instantaneous pollutant loads (mass of pollutant transported per unit time, L_i) were calculated as the product of instantaneous discharge and concentration. Most elements showed a similar temporal evolution, as typified by Zn in figure 6. For Zn, loads increased from 0.099 g/s on 02/10/04 to 23 g/s at the end of Event 1. The highest instantaneous loads occurred in Event 2 reaching peaks of 130 g/s in Event 2a and 820 g/s in Event 2b. By the end of Event 2c, field observations indicated that all of the salt minerals on the riverbanks had been dissolved and L_i had decreased to 21 g/s. The less pronounced increase in L_i observed in Event 3 was therefore not due to salt mineral dissolution from the riverbanks. Possible explanations include the dissolution of any remaining salt minerals within spoil heaps, the expellation of pore fluids from spoil heaps and increased mineral leaching during Event 3.

Differences between elements can be summarised by a ratio comparing peak L_i values in Event 2b and Event 3 (Peak 2b / Peak 3). For most elements, this ratio varies between 1.2 and 5.2 (Table 2). Elements with a ratio below 1 include Ca, K, Na, Si and Sr, all of which are present in the freshwater tributaries as well as the mining inputs. As with concentration profiles, Pb and Ba behave differently (Fig. 6). The highest measured L_i for each element occurred at the peak of Event 3 although it is also possible that similar peaks in L_i occurred in Event 2c but no samples were taken.

Total pollutant load estimations for October 2004 were calculated by establishing relationships between discharge and dissolved concentrations (Olías et al., 2006). Examples are shown in figure 7. Three different time periods were selected with good correlations: (1) from 20th October at 17:00 to 21st at 01:00 (the falling limb of Event 2b), (2) from 21st at 18:00 to 27th at 11:00 (the falling limb of Event 2c) and (3) from 27th at 14:00 onwards (Event 3). Where significant correlations ($p < 0.01$) were not established or datasets were incomplete, the pollutant load for each element was estimated as follows:

(i). From 1st October (00:00) to 9th October (08:00): discharge (4 L/s) was multiplied by time and the concentration of sample S1.

(ii). From 9th October (08:00) to 14th October (00:00): total discharge in the event was multiplied by the mean concentration of samples S1 and S2.

(iii). From 14th October (00:00) to 18th October (19:00): total discharge was multiplied by the concentration of sample S2.

(iv). From 18th October (19:00) to 20th October at 17:00, the following expression was applied:

$$L_T = \Sigma \tfrac{1}{2} (C_{i\ (n)} + C_{i\ (n+1)})\, Q_{T\ (n \rightarrow n+1)}$$

where L_T = total load, C_i = instantaneous concentration for sample n, Q_T = total discharge

Figure 7 also highlights an interesting comparison between the falling limbs of Event 2c and Event 3. Even though Event 2c was earlier in the month (and therefore may be expected to

405 have access to salt minerals and concentrated pore fluids), for many elements the falling limb of
406 the event had lower concentrations for any given discharge than the falling limb of Event 3. This
407 can be explained by the different rainfall distributions in each event. Figure 8 shows that the
408 rainfall maximum for Event 2c was located to the west of the mining area, leading to a large
409 input of diluting freshwater during this event. In contrast, Event 3 was focused on the mining
410 area itself. As mentioned in section 4.1, the higher rainfall in Event 3 combined with earlier
411 rainfall during the month meant that large inputs of freshwater from the Jarrama Reservoir did
412 flow into the river but not until the latter stages of the event, causing the stepped profile of the
413 falling limb (Fig. 2).
414
415 Table 4 compares the total loads estimated for October 2004 with September 2004 and with
416 previous estimates of annual loads. The total load for September 2004 was calculated using
417 sample S1 and a discharge of 0.004 m^3/s. This approach is justified as samples taken ~11 km
418 further downstream in September 2004 and early October 2004 showed little variation during
419 this time period (e.g. SO_4 = 1320 ± 69 mg/L, mean ± 1σ, n = 6). Overall the Río Tinto
420 transported approximately 1000 times more water in October 2004 than September 2004 and
421 between 140 (Na) and 8200 (Pb) times more dissolved elements, highlighting the extreme
422 seasonality of water flow and pollutant transport in this river and the key role of flood events.
423
424 In October 2004, 330 to 530 times more metals (Al, Cd, Co, Cr, Cu, Mg, Ni, Zn) and sulphate
425 than September 2004 were transported, with slightly higher values of Fe (770) and Mn (655).
426 The elements mobilised to the greatest degree by the additional water provided by the storm
427 events and tributaries were Pb (8200), As (5500), Ba (1900), Mo (1000) and K (880). If
428 anything, these values underestimate the total loads transported because only limited data was
429 available for Events 1 and 2c. During October 2004, Fe and Al were the dominant metals
430 transported by the Río Tinto followed by Cu, Zn and Mn with lesser quantities of toxic trace
431 elements such as Pb, Co, Ni, Li, Cd, As and Cr.
432

In this study, salt minerals were observed to have been dissolved by the end of Event 2. Events 1 and 2 combined transported approximately 58 t of Zn and 55 t of Cu. These estimates represent a possible upper limit for the amount of Zn and Cu stored by salt minerals in summer 2004, although as previously mentioned, neither Event 1 nor Event 2c were sampled in detail. In comparison, Buckby et al. (2003) extrapolated salt mineral coverage, density, porosity and chemical composition data to be 200 t of Zn and 150 t of Cu stored as salt minerals during the summer and dissolved by the first rainfall events of the autumn. The estimates by Buckby et al. (2003) and this study compare well, allowing for differences in the methodology used.

Extrapolating the data from September 2004 and October 2004 to create a yearly total is unwise given the inter- and intra-monthly variations in loads. Nevertheless, some comparisons can be made with previous estimations of annual metal loads (Table 4). Note the differences in the annual estimates. This is due to differences in both the years studied and the frequency of samples. Braungardt et al. (2003) extrapolated annual loads based on only 4 samples from different seasons in 1996-1998. The estimates for Sainz et al. (2004) were calculated in this study from their mean hourly loads (1988-2001). Sampling frequency was not given but appears to be quarterly. Finally, the estimates by Olías et al. (2006) were based on 419 samples collected between 1995 and 2003 (52 samples on average per year) and therefore are likely to be the most accurate published estimates.

Comparing the results of this study with Olias et al. (2006), it is striking that in October 2004 alone, almost 50% of the annual loads of Pb, Mn and Ni were transported to the Ría of Huelva estuary, once again highlighting the importance of flood events. At the other extreme, the As loads transported in October 2004 correspond to only 3 % of the annual total although Olias et al. (2006) did note that their As and Pb estimations had the highest uncertainties. These two elements showed the greatest difference between low-flow and flood regimes in this study.

4.5 Comparison with other AMD sites

462 Several studies have investigated the hydrochemical responses of small catchments affected by
463 AMD (Gammons et al., 2005; Lambing et al., 1999; Sanden et al., 1997; Wirt et al., 1999) while
464 the temporary storage of metals by salt mineral formation in dry periods followed by dissolution
465 and metal release by rainfall/flood events has been studied or proposed as an important
466 physicochemical process in a number of other works (Alpers et al., 1994; Bayless and Olyphant,
467 1993; Cravotta, 1994; Dagenhart, 1980; Hammarstrom et al., 2005; Keith et al., 2001).
468
469 Table 5 compares the characteristics of flood events in this study with Contrary Creek, Virginia
470 (Dagenhart, 1980) and Boulder Creek, Iron Mountain, California (Keith et al., 2001).
471 Instantaneous metal loads were calculated from discharge-time and concentration-time graphs.
472 Both of these studies displayed peaks in concentration associated with initial increases in
473 discharge followed by decreases in concentration as discharge continued to rise. It is clear from
474 these results that the Río Tinto represents the most extreme example of salt mineral dissolution
475 studied to date with the highest metal concentrations and loadings. Previous studies on the
476 adjacent Odiel River have calculated that it transports a higher dissolved load as it drains a
477 considerably larger catchment containing many mines. However, concentrations are much lower
478 and the pH is higher. Ongoing work at the University of Huelva is examining flood events in this
479 river using high-resolution temporal sampling.
480
481 In terms of the environmental impact on the estuary, elevated loads are arguably more
482 important than elevated concentrations in the Río Tinto, because concentrations are rapidly
483 diluted and pH increased as the Río Tinto water mixes with seawater and salinity increases in
484 the estuary (Braungardt et al., 2003). Higher loads may therefore cause elevated concentrations
485 to persist further into the estuary. Large, high-velocity discharges are also important because
486 they mobilise the highest amount of sediment, releasing metal-rich interstitial waters and
487 increasing concentrations still further in the upper Río Tinto Estuary (Braundgardt et al., 2003).
488 The key role of these events in the pollutant transport in arid and semi-arid environments should
489 be considered in all management strategies; these extreme variations in discharge and
490 concentrations complicate the design of effective treatment schemes in such climates.

491

492 **5. CONCLUSIONS**

493

494 This work is the first detailed investigation of the hydrochemical variations in the Río Tinto
495 during rainfall/flood events following a long dry season and it is likely the largest recorded
496 example of a flushout event in areas affected by AMD. Previous studies on the adjacent Odiel
497 River show a higher yearly dissolved load transported by this river. Ongoing work is examining
498 flood events and its impact on the metal load into the estuary.

499

500 As with previous studies examining rainfall events in AMD catchments (e.g. Dagenhart, 1980;
501 Keith et al., 2001), dissolved concentrations increased dramatically following the first rainfall
502 event of the season and then showed a general decrease throughout the month as the summer
503 store of soluble evaporitic salt minerals and concentrated pore waters was progressively
504 depleted and freshwater dilution processes became increasingly dominant.

505

506 Three separate rainfall/flood events were identified in the month. In general, concentrations
507 peaked following the first event (Q_{max} = 0.78 m^3/s) while dissolved loads peaked in the second
508 event (Q_{max} = 77 m^3/s) and discharge in the third event (Q_{max} = 127 m^3/s). Variations in relative
509 concentrations were attributed to oxyhydroxisulphate precipitation, to relative changes in the
510 sources of AMD (e.g. salt minerals, mine tunnels, spoil heaps etc.) and to a higher contribution
511 of freshwaters as the flood events progressed.

512

513 Ba and Pb behaved anomalously with concentrations and loads peaking at different times to
514 other elements. Ba behaviour could potentially be explained by equilibrium with a Ba-Sr
515 sulphate or by colloidal barite but there was no clear explanation for Pb.

516

517 Although significant ($p < 0.01$) relationships existed between discharge and concentrations for
518 certain periods, they could not be successfully extrapolated over the whole month or sometimes

519 over a whole event. This highlights the need for high-resolution temporal sampling of these
520 events in order to accurately estimate the annual dissolved load.
521
522 The dissolved pollutant load carried by the river during these floods was enormous. During
523 October 2004, some 5700 t of sulphates, 770 t of Fe, 420 t of Al, 100 t of Cu, 100 t of Zn and 71
524 t of Mn were transported by the Río Tinto into the Ría of Huelva estuary. Approximately 1000
525 times more water and 140-8200 times more dissolved elements were transported in October
526 2004 compared with the low-flow regime of September 2004. Total loads in October 2004
527 correspond to 3 % (As) to 46 % (Pb) of the annual loads estimated by Olías et al. (2006)
528 although more accurate annual loads (in dry and wet years) involving detailed sampling of flood
529 events are needed to properly assess the contribution of flood events.
530

531 Acknowledgements

532

533 The authors wish to thank the Guadiana Hydrographic Confederation, and the Environmental
534 Council of the Andalusia Regional Government for the information provided for this study, which
535 has been financed through the project “Mining contamination evaluation, acid mine drainage
536 treatment, hydrologic modelling of the Odiel River basin and study of the contaminant load to
537 the Huelva estuary”, financed by the Environmental Council of the Andalusia Regional
538 Government, and CTM2006-28148-E/TECNO - CTM2007-66724-C02-02/TECNO financed by
539 the Spanish Ministry of Education and Science. Chris Hubbard was funded by a University of
540 Reading Postgraduate Studentship.
541

542 References

543

544 Acero, P., Ayora, C., Torrentó, C., Nieto, J.M., 2006. The behaviour of trace elements during
545 schwertmannite precipitation and subsequent transformation into goethite and jarosite.
546 Geochimica et Cosmochimica Acta, 70, 4130-4139.

547 Achterberg, E.P., Herzl, V.M.C., Braungardt, C.B., Millward, C.E., 2003. Metal behaviour in an
548 estuary polluted by acid mine drainage: the role of particulate matter. Environmental
549 Pollution, 121, 283-292.
550 Alpers, C.N., Nordstrom, D.K., Thompson, J.M., 1994. Seasonal variations of Zn/Cu ratios in
551 acid-mine water from Iron-Mountain, California, in: Alpers, C.N., Blowes, D.W. (eds.),
552 Environmental geochemistry of sulfide oxidation. ACS Symposium Series 550, pp 324-
553 344.
554 Ball, J.W., Nordstrom, D.K., 1991. WATEQ4F—User's manual with revised thermodynamic data
555 base and test cases for calculating speciation of major, trace and redox elements in
556 natural waters. U.S. Geological Survey Open-File Report 90–129, 185 p.
557 Bayless, E.R., Olyphant, G.A., 1993. Acid-generating salts and their relationship to the
558 chemistry of groundwater and storm runoff at an abandoned mine site in southwestern
559 Indiana, USA. Journal of Contaminant Hydrology, 12, 313-328.
560 Bigham, J.M, Schwertmann, U., Traina, S.J., Winland, R.L., Wolf., M., 1996. Schwermannite
561 and the chemical modeling of iron in acid sulfate waters. Geochimica et Cosmochimica
562 Acta, 60, 2111-2121.
563 Boyle, E.A., Chapnick, S.D., Bai, X.X., Spivack, A., 1985. Trace-metal enrichments in the
564 Mediterranean Sea. Earth and Planetary Science Letters, 74, 405-419.
565 Boyle, E.A., Huested, S.S, Grant, B., 1982. The chemical mass-balance of the Amazon plume:
566 II,Copper, Niquel and Cadmium. Deep Sea Research, 29, 1355-1364.
567 Braungardt, C.B., Achterberg, E.P., Elbaz-Poulichet, F., Morley, N.H., 2003. Metal geochemistry
568 in a mine polluted estuarine system in Spain. Applied Geochemistry, 18, 1757-1771.
569 Buckby, T., Black, S., Coleman, M.L., Hodson, M.E., 2003. Fe-sulphate rich evaporative mineral
570 precipitates from the río Tinto, southwest Spain. Mineralogical Magazine, 67 (2), 263-278.
571 Cánovas, C.R, Olias, M., Nieto, J.M, Sarmiento, A.M, Cerón, J.C, (2007): Hydrogeochemical
572 characteristics of the Odiel and Tinto rivers (SW Spain). Factors controlling metal
573 contents. Science of the Total Environment, 373, 363-382.
574 Chapman B.M., Jones D.R., Jung R.E., 1983. Processes controlling metal ion attenuation in
575 acid mine drainage streams, Geochimica et Cosmochimica Acta 47, 1957-1973.

576 Cravotta, C.A., 1994. Secondary iron-sulfate minerals as sources of sulphate and acidity –
577 geochemical evolution of acidic ground-water at a reclaimed surface coal-mine in
578 Pennsylvania, in: Alpers, C.N., Blowes, D.W. (eds.), Environmental geochemistry of
579 sulfide oxidation. ACS Symposium Series 550. 345-364.
580 Dagenhart, T.V. Jr., 1980. The acid mine drainage of Contrary Creek, Louisa County, Virginia:
581 Factors causing variations in stream water chemistry. MSc thesis, Univ. Virginia,
582 Charlottesville, Virginia.
583 Drever, J.I., 1997. The Geochemistry of natural waters : surface and groundwater environments.
584 Prentice Hall, New Jersey, 437 p.
585 Elbaz-Poulichet, F., Morley, N.H., Cruzado, A., Velasquez, Z., Achterberg, E. P., Braungardt,
586 C.B., 1999. Trace metal and nutrient distribution in an extremely low pH (2.5) river-
587 estuarine system, the Ria of Huelva (South-West Spain). Science of the Total
588 Environment, 227, 73-83.
589 Elbaz-Poulichet, F., Braungardt, C., Achterberg, E., Morley, N., Cossa, D., Beckers, J.,
590 Nomérange, P., Cruzado, A., Leblanc, M., 2001. Metal biogeochemistry in the Tinto-Odiel
591 rivers (Southern Spain) and in the Gulf of Cadiz: a synthesis of the results of the TOROS
592 project. Continental Shelf Research, 21, 1961-1973.
593 Elbaz-Poulichet, F., Seidel, J.L., Casiot, C., Velasquez, Z., Tusseau-Vuillemin, M.H., 2006.
594 Short-term variability of dissolved trace element concentrations in the Marne and Seine
595 Rivers near Paris. Science of the Total Environment, 367, 278-287.
596 Fernández-Remolar, D., Rodriguez, N., Gómez, F., Amils, R., 2003. Geological record of an
597 acidic environment driven by iron hydrochemistry: The Tinto River system. Journal of
598 Geophysical Research, 108 (E7), Art. No. 5080.
599 Fernández-Remolar, D., Gómez-Elvira, J., Gómez, F., Sebastián, J., Martín, J., Manfredi, J.A.,
600 Torres, J., González Kessler, C., Amils, R., 2004. The Tinto river, an extreme acidic
601 environment under control of iron, as an analog of the Terra Meridiani hematite site of
602 Mars. Planetary and Space Science, 52, 239-248.
603 Fernández-Remolar, D., Morris, R.V., Gruener, J.E., Amils, R., Knoll, A.H., 2005. The Río Tinto
604 Basin, Spain: Mineralogy, sedimentary geobiology, and implications for interpretation of

outcrop rocks at Meridiani Planum, Mars. Earth and Planetary Science Letters, 240, 149-167.

Ferris, F.G.,Hallbeck, L., Kennedy, C.B., Pedersen, K., 2004. Geochemistry of acidic Rio Tinto headwaters and role of bacteria in solid phase metal partitioning. Chemical Geology, 212, 291-300.

Galán, E., Gómez-Ariza, J.L., González, I., Fernández-Caliani, J.C., Morales, E., Giráldez, I., 2003. Heavy metal partitioning in river sediments severely polluted by acid mine drainage in the Iberian Pyrite Belt. Applied Geochemistry, 18, 409-421.

Gammons, C.H., Shope, C.L., Duaime, T.E., 2005. A 24 h investigation of the hydrogeochemistry of baseflow and stormwater in an urban area impacted by mining: Butte, Montana. Hydrological Processes, 19, 2737-2753.

González-Toril, E., Llobet-Brossa, E., Casamajor, E.O., Amann, R., Amils, R., 2003a. Microbial ecology of an extreme acidic environment, the Tinto River. Applied and Environmental Microbiology, 69, 4853-4865.

González-Toril, E., Gómez, F., Rodríguez, N., Fernández Remolar, D., Zuluaga., J., Marín, I., Amils, R., 2003b. Geomicrobiology of the Tinto River, a model of interest for biohydrometallurgy. Hydrometallurgy, 71, 301-309.

Hammarstrom, J.M., Seal, R.R., Meier, A.L., Kornfeld, J.M., 2005. Secondary sulfate minerals associated with acid drainage in the eastern US: recycling of metals and acidity in surficial environments. Chemical Geology, 215, 407-431.

Hubbard, C. G., 2007. Acid mine drainage generation and transport processes in the Tinto River, SW Spain. PhD thesis. University of Reading, UK.

Hudson-Edwards,K.A., Schell, C., Macklin, M.G., 1999. Mineralogy and geochemistry of alluvium contaminated by metal mining in the Rio Tinto area, southwest Spain. Applied Geochemistry, 14, 1015-1030.

Keith, D.C., Runnells, D.D., Exposito, K.J., Chermak, J.A., Levy, D.B., Hannula, S.R., Watts, M., Hall, L., 2001. Geochemical models of the impact of acidic groundwater and evaporative sulphate salts on Boulder Creek at Iron Mountain, California. Applied Geochemistry, 16, 947-961.

634 Lambing, J.H., Nimick, D.A., Cleasby, T.E., 1999. Short-term variation of trace-element
635 concentrations during base flow and rainfall runoff in small basins. U.S. Geological
636 Survey. Open-File Report 99-159. 32 p.
637 Leblanc, M., Morales, J.A., Borrego. J., Elbaz-Poulichet, F., 2000. 4.500 year old mining
638 pollution in Southwestern Spain: long-term implications for modern mining pollution.
639 Economical Geology, 95, 655-662.
640 Lee, J.H., Bang, K.W., 2000. Characterization of urban stormwater runoff. Water Research, 34,
641 1773-1780.
642 Lee, G., Bigham, J.M., Faure, G., 2002. Removal of trace metals by coprecipitation with Fe, Al
643 and Mn from natural waters contaminated with acid mine drainage in the Ducktown
644 Mining District, Tennessee. Applied Geochemistry, 17, 569-581.
645 López-Archilla, A.I., Marin, I., Amils, R., 2001. Microbial community composition and ecology of
646 an acidic aquatic environment: The Tinto River, Spain. Microbial Ecology, 41, 20-35.
647 López-Archilla, A.I., Gérard, E., Moreira, D., López-García, P., 2004. Macrofilamentous
648 microbial communities in the metal rich and acidic river Tinto, Spain. FEMS Microbiology
649 Letters, 235, 221-228.
650 López-González, N., Borrego, J., Morales, J.A., Carro, B., Lozano-Soria, O., 2006. Metal
651 fractionation in oxic sediments of an estuary affected by acid mine drainage (south-
652 western Spain). Estuarine, Coastal and Shelf Science, 68, 297-304.
653 Lottermoser, B.G., 2005. Evaporative mineral precipitates from a historical smelting slag dump,
654 Río Tinto, Spain. Neues Jahrbuch für Mineralogie - Abhandlungen, 181/2, 183-190.
655 Malki, M., González-Toril, E., Sanz, J.L., Gómez, F., Rodríguez, N., Amils, R., 2006. Importance
656 of the iron cycle in biohydrometallurgy. Hydrometallurgy, 83, 223-228.
657 Naus, C.A., McCleskey, R.B., Nordstrom, D.K., Donohoe, L.C., Hunt, A.G., Paillet, F.L., Morin,
658 R.H., and Verplanck, P.L., 2005, Questa Baseline and Pre-Mining Ground-Water-Quality
659 Investigation. 5. Well Installation, Water-Level Data, and Surface- and Ground-Water
660 Geochemistry in the Straight Creek Drainage Basin, Red River Valley, New Mexico,
661 2001-03: U.S. Geological Survey Scientific Investigations Report 2005-5088, 220 p.

662 Neal, C., Jarvie, H.P., Whitton, B.A., Gemmell, J., 2000. The water chemistry of the River Wear,
663 north-east England. Science of the Total Environment, 251/252, 153-172.
664 Nieto, J.M, Sarmiento, A.M, Olias, M., Cánovas, C.R., Riba, I, Kalman, J, Delvalls, T.A. 2007.
665 Acid mine drainage pollution in the Odiel and Tinto rivers (Iberian Pyrite Belt, SW Spain)
666 and bioavailability of the transported metals to the Huelva estuary. Environment
667 International, 33, 445-455.
668 Nocete, F., Alex, E., Nieto, J.M., Sáez, R., Bayona, M.R., 2005. An archaelogical approach to
669 regional environmental pollution in the south-western Iberian Peninsula related to Third
670 Millenium B.C mining and metallurgy. Journal of Archaelogical Science, 32, 1566-1576.
671 Nordstrom, D.K., Alpers, C.N., 1999. Geochemistry of acid mine waters, in: Plumlee, G.S. and
672 Logson, M.J (eds.), The environmental geochemistry of mineral deposits. Rev. Econ.
673 Geol. 6A, 133-160.
674 Olías, M., Cánovas, C.R., Nieto. J.M., Sarmiento, A.M., 2006. Evaluation of the dissolved
675 contaminant load transported by the Tinto and Odiel rivers (South West Spain). Applied
676 Geochemistry, 21, 1733-1749.
677 Parkhurst, D.L., Appelo, C.A.J., 1999. User's guide to PHREEQC (Version 2) - A computer
678 program for speciation, batch reaction, one-dimensional transport, and inverse
679 geochemical calculations. USGS Water-Resources Investigations Report 99-4259.
680 Denver, USA. 312 p.
681 Ruiz, F., González-Regalado, M.L., Borrego, J., Morales, J.A., Pendón, J.G., Muñoz, J.M.,
682 1998. Stratigraphic sequence, elemental concentrations and heavy metal pollution in
683 Holocene sediments from the Tinto-Odiel Estuary, southwestern Spain. Environmental
684 Geology, 34 (4), 270-278.
685 Ruiz, M.J., Carrasco, R., Pérez, R., Sarmiento, AM., Nieto, J.M., 2003. Optimización del análisis
686 de elementos mayores y traza mediante UN-ICP-OES en muestras de drenaje ácido de
687 mina. Proceedings IV Iberian Geochemical Meeting, 14-18 Julio. Coimbra, Portugal.
688 Universidad de Coimbra. 402–404.
689 Sainz, A., Grande, J. A., De La Torre, M. L., 2004. Characterisation of heavy metal discharge
690 into the Ria of Huelva. Environment International, 30, 557-566.

691 Sandén, P., Karlsson, S., Düker, A., Ledin, A., Lundman, L., 1997. Variations in hydrochemistry,
692 trace metal concentration and transport during a rain storm event in a small catchment.
693 Journal of Geochemical Exploration, 58, 144-155.
694 Sarmiento, A.M., Nieto, J.M., Olías, M., 2004. The contaminant load transported by the river
695 Odiel to the Gulf of Cádiz (SW Spain). Applied Earth Science : IMM Transactions section
696 B, 113, 117-122
697 Smith, K.S., 1999. metal sorption on mineral surfaces: an overview with examples relating to
698 mineral deposits, in: Plumlee, G.S. and Logson, M.J (eds.), The environmental
699 geochemistry of mineral deposits. Rev. Econ. Geol. 6A, 161-182.
700 Stumm, W., Morgan, J., 1996. Aquatic chemistry: chemical equilibria and rates in natural
701 waters. John Willey and Sons. New York, 1022 p.
702 Thevenot, D.R., Moilleron, D., Lestel, L., Gromaire, M.C., Rocher, V., Cambier, P., Bonte, P.,
703 Colin, J.L., de Ponteves, C., Meybeck., M., 2007. Critical budget of metal sources and
704 pathways in the Seine River basin (1994-2003) for Cd, Cr, Cu, Hg, Ni, Pb and Zn.
705 Science of the Total Environment, 375, 180-203.
706 Tornos, F., 2006. Environment of formation and styles of volcanogenic massive sulfides: The
707 Iberian Pyrite belt. Ore Geology Reviews, 28, 259-307.
708 van Geen, A., Boyle, E.A., Moore, W.S., 1991. Trace-metal enrichments in waters of the Gulf of
709 Cadiz, Spain. Geochimica et Cosmochimica Acta, 55, 2173-2191.
710 van Geen, A., Adkins, J.F., Boyle, E.A., Palanques, A., 1997. A 120 year record of widespread
711 contamination from mining of the Iberian Pyrite Belt. Geology, 25, 291-294.
712 Vink, R., Behrendt, H., Salomons, W., 1999. Development of the heavy metal pollution trends in
713 several European rivers: An analysis of point and diffuse sources. Water Science and
714 Technology, 39, 215-223
715 Walling, D.E., Foster, D.E., 1975. Variations in the natural chemical concentration of river water
716 during flood flows, and the lag effect: some further comments. Journal of Hydrology, 26,
717 237-244.
718 World Health Organisation (WHO), 2004. Guidelines for drinking-water quality, 3rd edition.
719 Geneva.

720 Wirt, L., Leib, K.J., Bove, D.J., Mast, M.A., Evans, J.B., Meeker, G.P., 1999. Determination of
721 Chemical-Constituent Loads During Base-Flow and Storm-Runoff Conditions Near
722 Historical Mines in Prospect Gulch, Upper Animas River Watershed, Southwestern
723 Colorado. U.S. Geological Survey. Open File Report 99-159.
724 Yu, J.Y., Heo, B., Choi, I.K., Cho, J.P., Chang, H.W., 1999. Apparent solubilities of
725 schwertmannite and ferrydrite in natural stream waters polluted by mine drainage.
726 Geochimica et Cosmochimica Acta, 63, 3407-3416.
727 Zänker, H., Moll, H., Richter, W., Brendler, W., Hennig, C., Reich, T., Kluge, A., Hüttig, G., 2002.
728 The colloid chemistry of acid rock drainage solution from an abandoned Zn-Pb-Ag mine.
729 Applied Geochemistry 17, 633-648.
730 Zettler, L.A.A., Gomez, F., Zettler, E., Keenan, B.G., Amils, R., Sogin, M.L., 2002. Eukaryotic
731 diversity in Spain's river of fire. Nature, 417, 137-137.

Figures

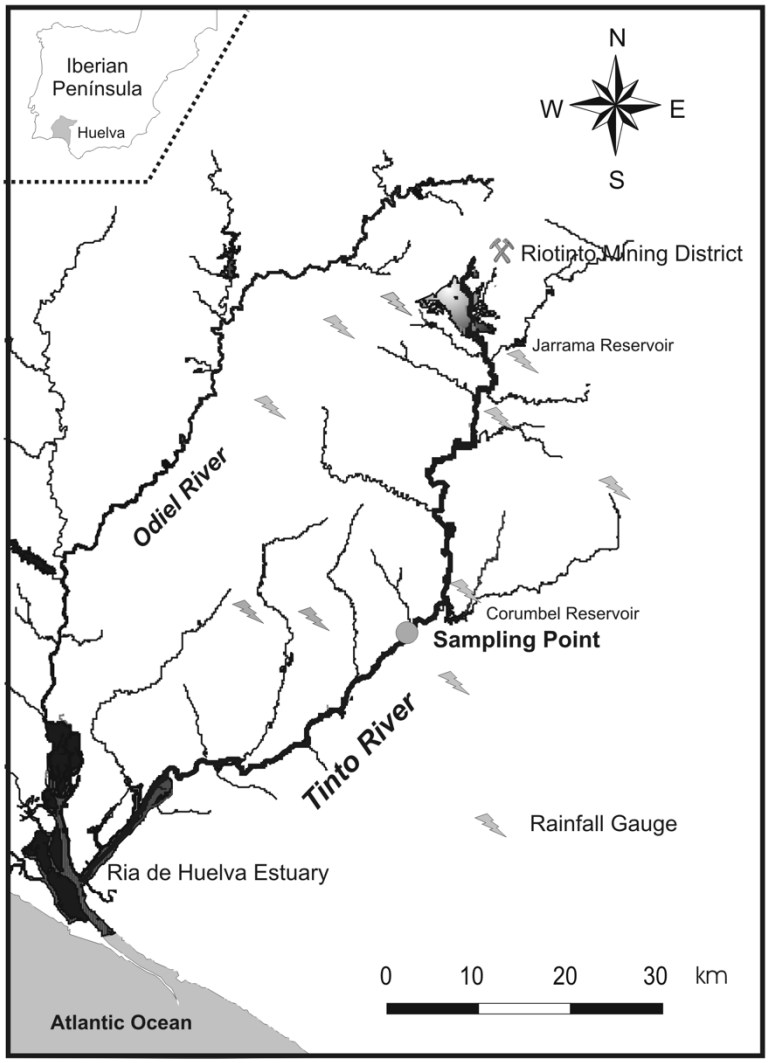

Figure 1. Map of the Río Tinto showing the location of the sampling point, the mining area and the pluviometric gauges.

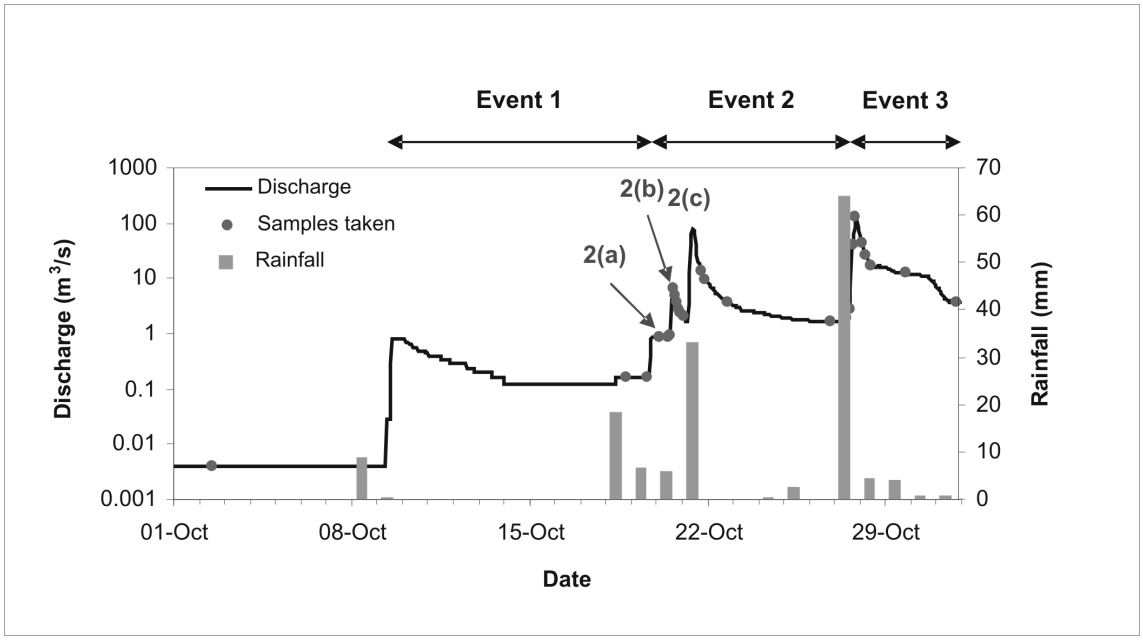

Figure 2. Rainfall and discharge data for the monitored period.

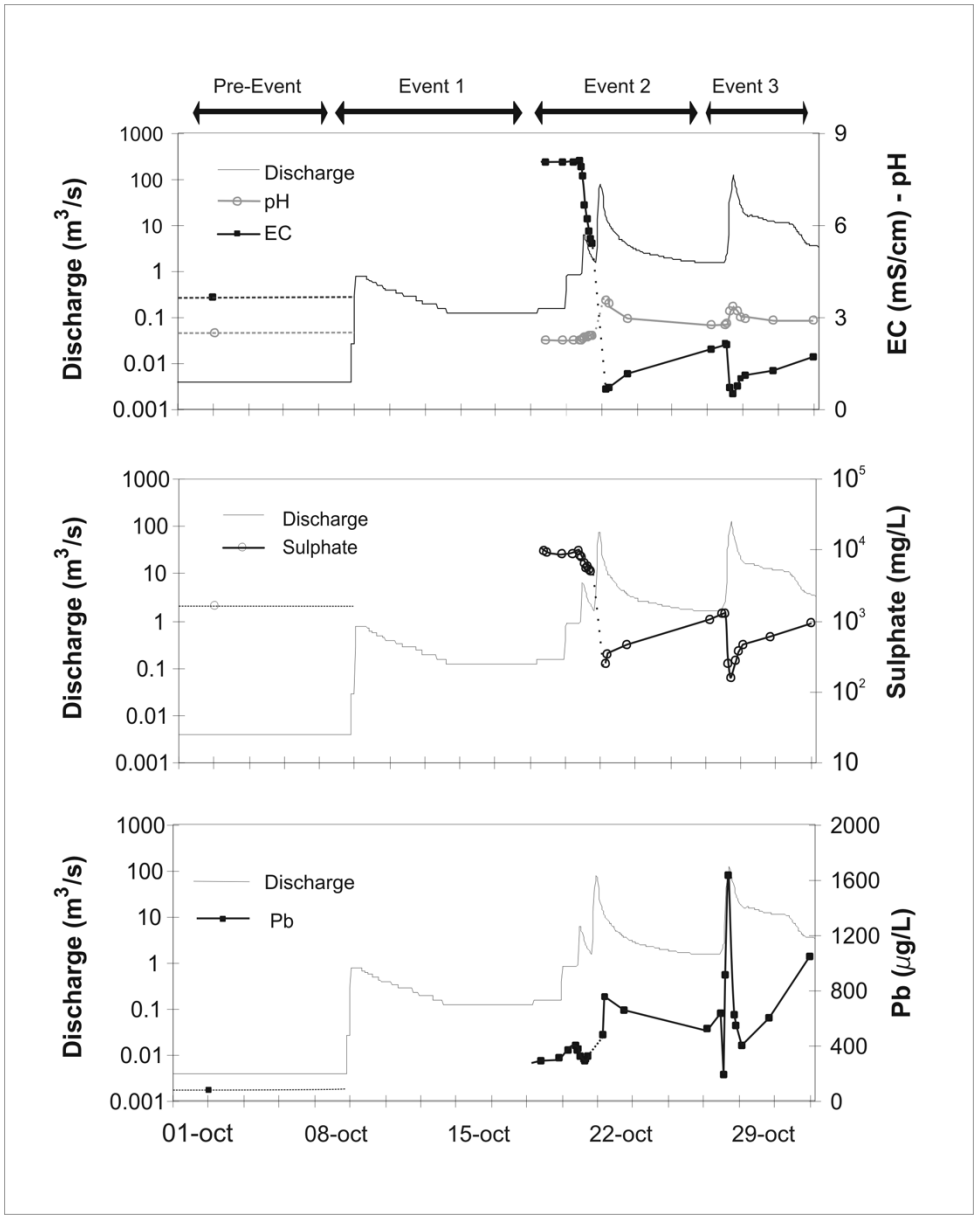

Figure 3. Variations in pH, electrical conductivity and sulphate and Pb dissolved concentrations.

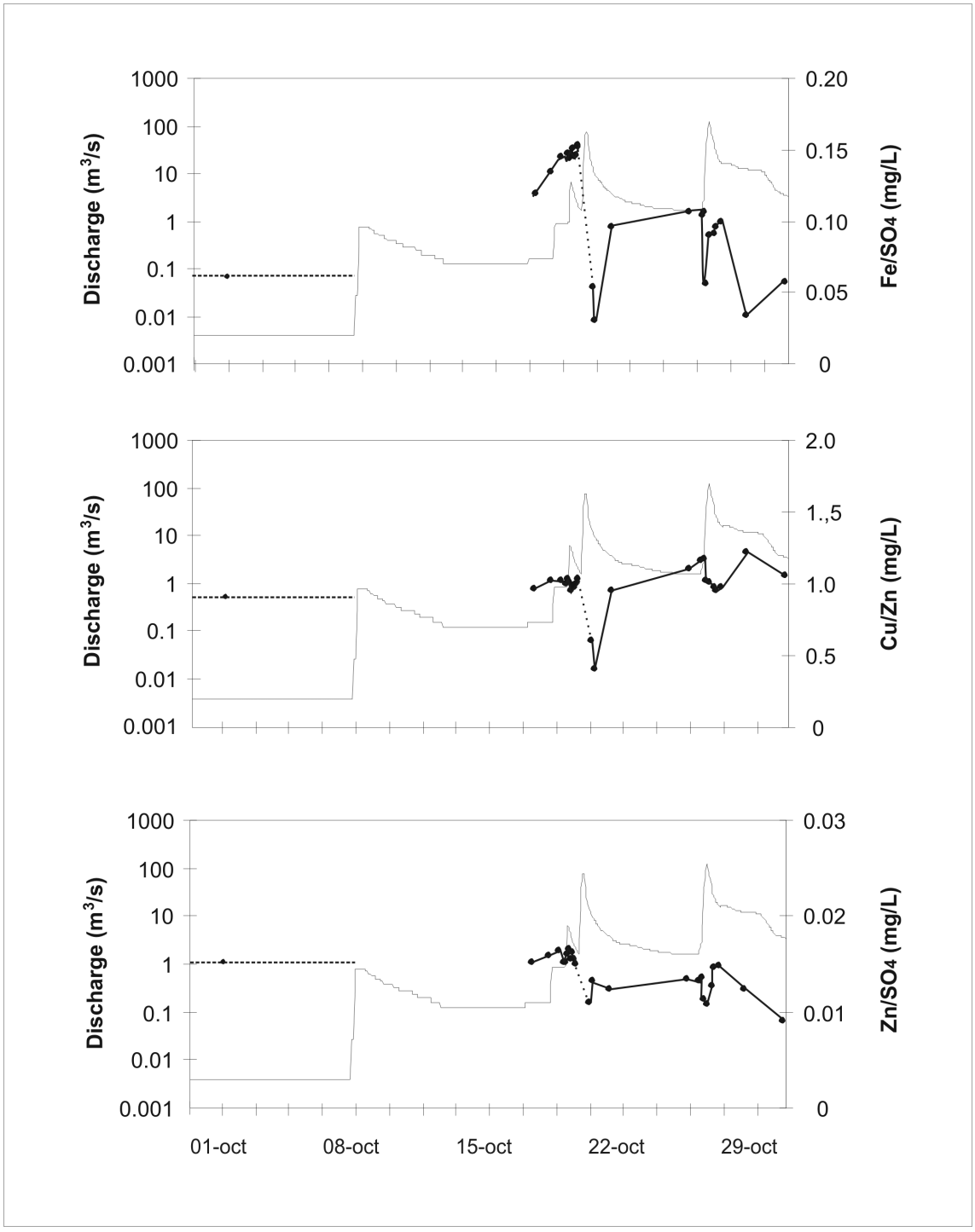

Figure 4. Variations in Fe/SO_4, Cu/Zn and Zn/SO_4 ratios.

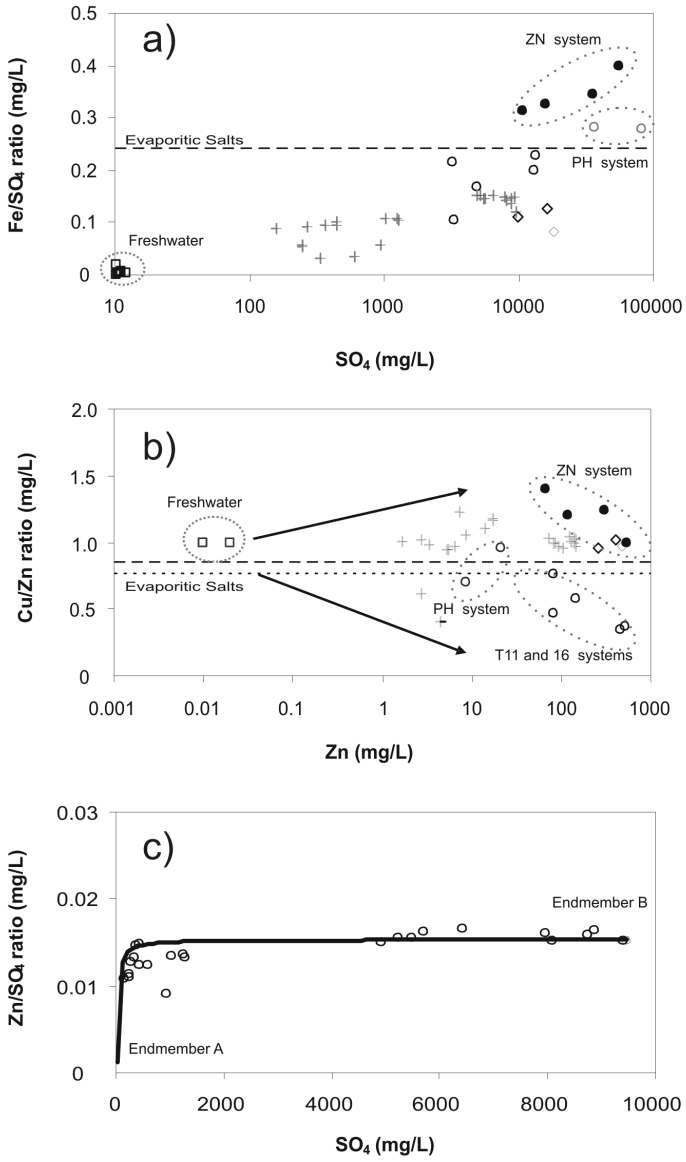

Figure 5. a) Fe/SO_4 ratio *versus* SO_4 concentration; b) Cu/Zn ratio *versus* SO_4 concentration; c) Zn/SO_4 versus SO_4 concentration showing a mixing line between freshwater (end-member A) and the most contaminated sample (end-member B). *Ionic ratio from evaporitic salts expressed as the median value from Buckby et al., 2004 (dashed line) and from this study (pointed line). AMD sources: Zarandas Naya System (ZN System), Tunnel 11 and 16 systems (T11 and T16) and Peña del Hierro system (PH system). Freshwater data are from the Corumbel reservoir.*

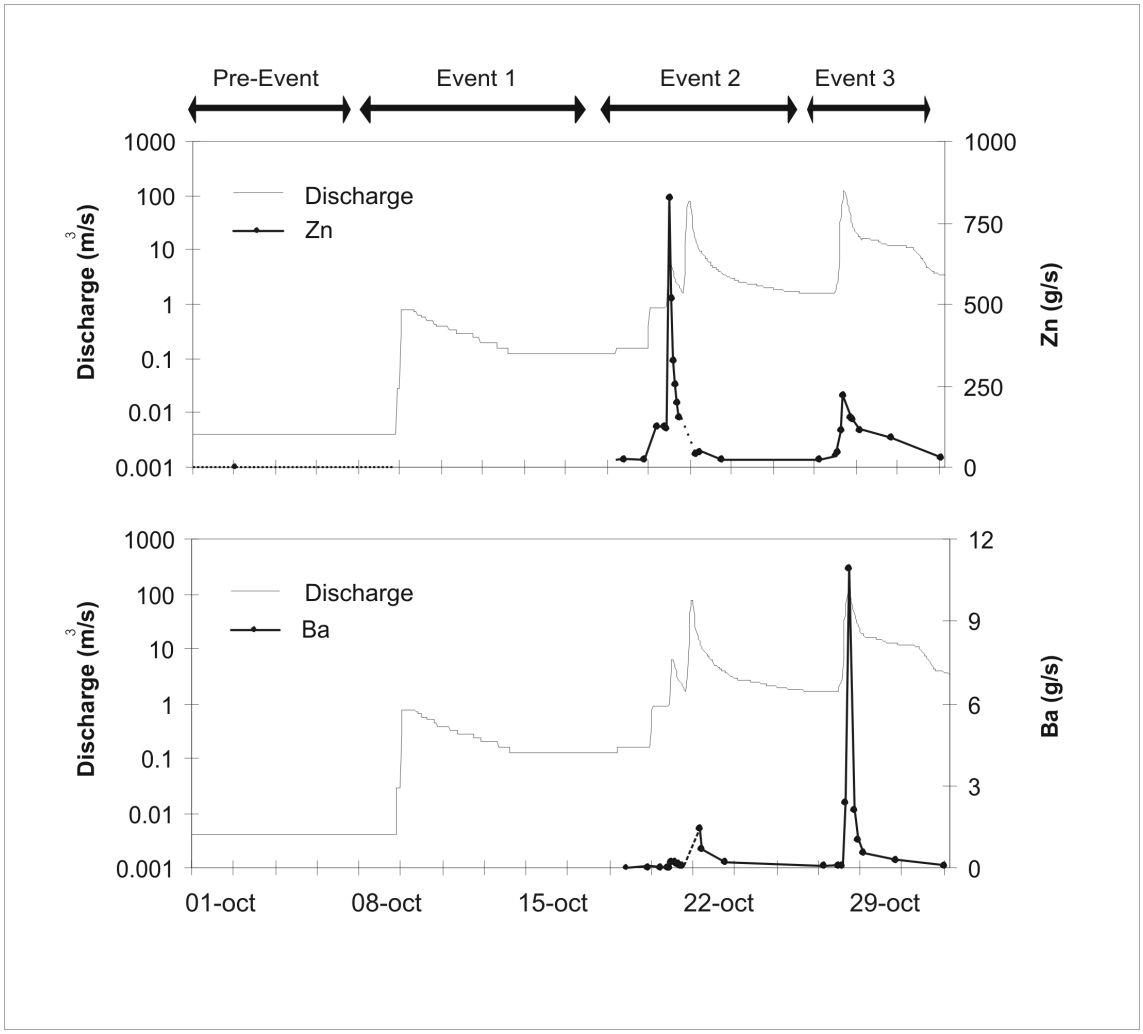

Figure 6. Instantaneous dissolved loads of Zn and Ba.

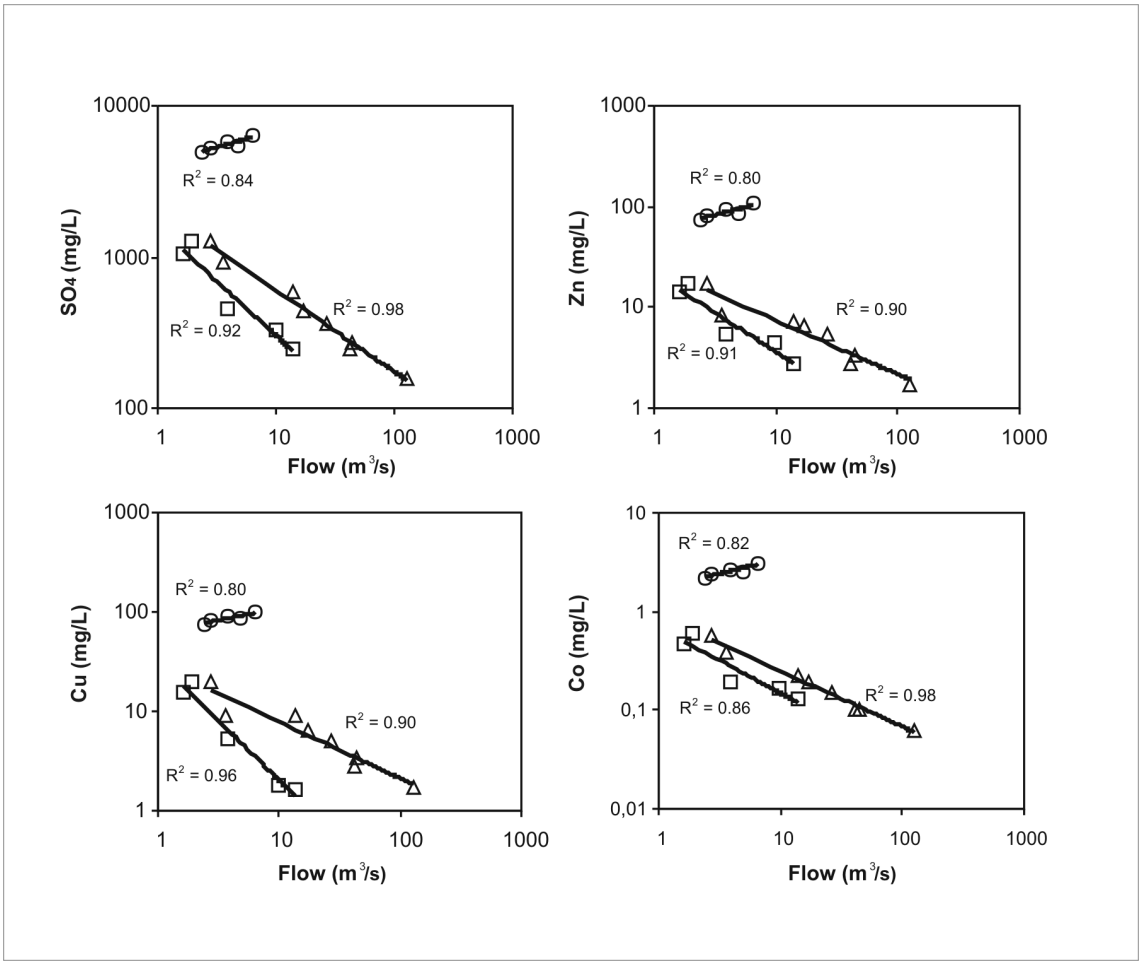

Figure 7. Examples of relationships between discharge and dissolved concentrations during October 2004 (circles = from 20th at 17:00 to 21st at 01:00; squares = from 21st at 18:00 to 27th at 11:00; and triangles = from 27th at 14:00 on).

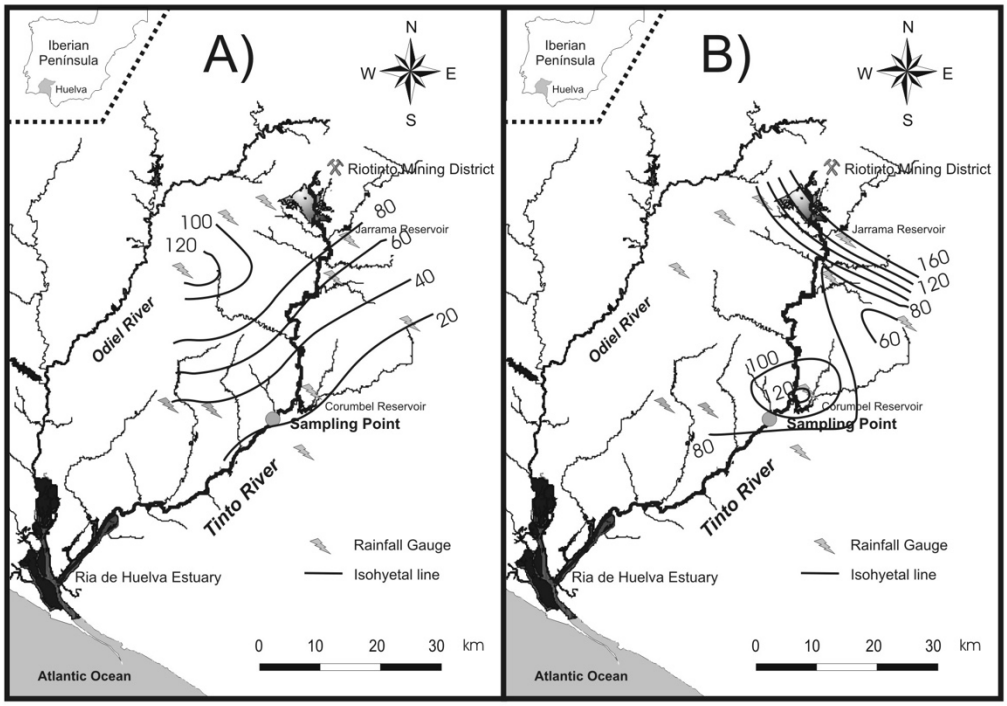

Figure 8. Rainfall distribution in the Río Tinto basin during: a) Event 2; b) Event 3.

River	Catchment	Discharge	Al	As	Cd	Cu	Fe	Mn	Pb	Zn
	km²	*m³/s*	*Dissolved concentrations (mg/L)*							
Río Tinto [1]	***1646***	***1.6***	***75***	***0.86***	***0.25***	***27.2***	***393***	***11.4***	***0.19***	***61.8***
Thames [2]	12935	65.8		0.003		0.004		0.1	<0.001	
Seine [3]	78650	435		0.001	0.03	0.002		0.006	<0.001	
Rhone [4]	159127	2170		0.002	0.03	0.002			<0.001	
Mississippi [5]	2981000	12743			<0.001	0.02				0.003
Amazon [4]	7050000	219000			0.06	0.02				<0.004
Streams average [6]			0.05	0.002		0.007	0.04	0.008	0.001	0.03
			Annual Load (ton / yr)							
Río Tinto [1]	***1646***	***1.6***	***1234***	***12.4***	***3.9***	***469***	***5075***	***163***	***14.8***	***863***
Seine [7]	78650	435			0.44	25			9	135
Elbe [8]	131950	720		16.3	2.5	51.4			22.8	501
Rhone [8]	159127	2170		40.4	2.5	149.5			225.9	966

1. Olias et al., 2006 2. Neal et al., 2000 3. Elbaz Poulichet e al., 2006 4. Boyle et al., 1982
5. Stumm and Morgan, 1996 6. Drever, 1988 7. Thévenot et al., 2007 8. Vink et al., 1999.

Table 1. Element concentrations and loads transported by rivers worldwide.

		n	*Mean*	*Median*	*Stand. Deviat.*	*Min.*	*Max.*	*Percentile 25*	*Percentile 75*	*Peak 2b / Peak 3*	*Detect. limit*
Flow	**m³/s**	25	12.5	3.7	20.6	0.004	87.3	1.46	13.7		
pH		25	2.70	2.75	0.42	2.25	3.56	2.31	2.95		
EC	**mS/cm**	25	3.87	2.13	3.02	0.51	8.08	1.11	6.67		
Eh	**mV**	25	726	735	74	608	840	664	783		
Main eleme.	**SO_4**	25	3583	1272	3572	158	9474	443	6437	2.5	0.09
	Al	25	192	82	186	7.0	483	26	343	3.1	0.06

	Ca	25	86	43	69	13	184	24	151	0.6	0.06
	Cu	25	55	20	57	1.6	148	5	102	3.8	0.08
	Fe	25	489	133	522	10	1385	35	969	4.2	0.03
	K	25	2.7	1.9	2.1	0.6	8.5	1.3	3.2	0.03	0.06
	Mg	25	184	67	179	10	463	24	343	2.2	0.08
	Mn	25	25	12	21	2.1	56	5	47	1.2	0.07
	Na	25	28	16	22	6.2	64	8	49	0.4	0.08
	Si	25	25	15	22	3.9	69	5	39	0.6	0.02
	Zn	25	55	17	57	1.7	145	6	107	3.8	0.14
Trace elements (µg/L)	**As**	25	316	40	349	6	879	12	651	5.2	2.73
	Ba	24	40	35	23	13	104	24	46	0.02	0.20
	Be	20	10	12	8	1.3	23	3	17	1.4	1.10
	Cd	25	274	82	283	9	740	25	507	3.4	1.31
	Co	25	1618	602	1616	62	4142	191	3091	3.0	1.94
	Cr	25	60	15	64	1.3	181	3	113	4.9	1.75
	Li	25	320	276	291	13	803	41	568	2.5	1.55
	Mo	24	49	13	48	1.5	131	8	91	3.8	2.31
	Ni	25	493	226	493	23	1279	55	926	2.4	1.22
	P	24	550	518	499	28	1191	50	1021	1.8	7.04
	Pb	25	508	402	322	80	1637	313	619	0.01	2.20
	Sn	23	54	12	52	0.9	130	7	106	24	0.55
	Sr	25	219	138	153	39	483	84	334	0.04	0.07

Table 2. Basic statistics of results obtained during the flood events

		CH68	CH71	CH73	CH74	CH75	CH157	CH163	CH179	CH204	CH209	C
Location		7.2	7.2	8.2	8.2	8.2	79	21	0.2	7.2	7.2	
Mineralogy		Cp, Ha, Hx, Gyp	Rz, Cp, Ha, Hx	Me, Pi, Gyp, Jt	Sz, Rh, Al	FeCp, AlCp		Hx, Ha, Cp, S	Cp, Cq, Al	Ha	Rz, AlCp, Gu, Gyp	Rz C
Fe	%	6.85	12.4	29.1	21.4	23.2	0.42	2.78	17.1	0.32	20.3	
Mg	%	3.20	5.08	0.28	0.23	0.17	4.26	6.40	2.11	2.69	4.11	
Al	%	3.63	2.57	0.52	2.40	1.00	3.47	2.67	2.45	4.60	0.31	
Na	%	0.59	0.22	0.16	0.26	0.10	3.41	0.74	0.04	0.24	0.16	
Mn	%	0.43	0.64	0.05	0.05	0.05	0.57	0.66	0.03	0.43	0.62	
Ca	%	0.29	< 0.009	0.11	0.01	< 0.009	0.06	< 0.009	< 0.009	< 0.009	0.19	
Si	%	0.22	< 0.005	< 0.005	< 0.005	< 0.005	< 0.005	< 0.005	< 0.005	< 0.005	< 0.005	<
Ti	%	0.01	< 0.003	< 0.003	0.01	< 0.003	< 0.003	0.01	< 0.003	< 0.003	< 0.003	<
P	%	0.013	< 0.003	< 0.003	0.013	0.004	0.004	0.004	< 0.003	< 0.003	< 0.003	<
K	%	< 0.01	< 0.01	< 0.01	< 0.01	< 0.01	< 0.01	< 0.01	< 0.01	< 0.01	< 0.01	
Zn	mg/kg	11300	4900	5240	4750	5510	17500	12100	183	13800	7060	
Cu	mg/kg	12200	765	4590	3380	4350	4850	5790	173	11800	257	
Co	mg/kg	375	236	102	78	86	419	325	181	374	333	
Pb	mg/kg	32	15	118	25	11	bdl	13	10	41	256	
Ni	mg/kg	98	41	25	29	23	81	152	13	36	24	
Zr	mg/kg	16	< 5	13	27	12	20	12	6	18	13	
Cr	mg/kg	< 5	5	12	29	23	27	8	10	< 5	8	
V	mg/kg	< 2	7	17	36	15	< 2	15	7	< 2	10	
Y	mg/kg	17	6	< 5	10	< 5	27	23	8	19	< 5	
Sr	mg/kg	6	8	< 5	< 5	< 5	< 5	7	< 5	< 5	13	
Rb	mg/kg	< 5	< 5	< 5	< 5	< 5	10	< 5	< 5	< 5	< 5	

Al = alunogen, AlCp = aluminocopiapite, Cp = copiapite, Cq = coquimbite, FeCp = ferricopiapite, Gu = gunningite, Gyp = gy
Hx = hexahydrite, Jt = jarosite, Me = melanterite, Pi = pisanite, Qz = quartz, Rh = rhomboclase, Rz = rozenite, S = NaAl(SO
S = $NaAl(SO_4)_2.12H_2O$ (syn), Sz = szomolnokite.
Location: distance downstream from source (km)

Table 3. Mineralogy and chemistry of salt minerals collected in August 2003 (CH68-CH75) and September 2004 (CH157-CH260)

	Braungardt 1 Year	Sainz 1 Year	Olías 1 Year	This study Sept. 2004	This study Octob. 2004	This study as % of Olías
Al	-	-	1224	0.92	420	34
As	-	9.5	12.4	0.0001	0.41	3.3
Ba	-	-	-	0.0004	0.70	-
Cd	0.86	2.8	3.9	0.0013	0.49	13
Co	3.3	-	8.7	0.0071	3.3	38
Cr	-	1.4	-	0.0002	0.10	-
Cu	88	284	469	0.23	100	21
Fe	1540	-	5075	1.0	770	15
Li	-	-	-	0.0029	0.58	-
Mn	61	85	163	0.11	71	44
Ni	1.4	2.7	2.2	0.0023	1.0	45
Pb	0.87	1.8	14.8	0.0008	6.8	46
SO_4	-	-	36589	17	5700	16
Zn	240	596	863	0.26	100	12

Braungardt et al. (2003), Sainz et al. (2004), Olías et al. (2006)

Table 4. Pollutant load estimates for the Río Tinto (tonnes)

	Río Tinto This study	**Boulder Creek** Keith et al. (2001)	**Contrary Creek** Dagenhart (1980)
Q_{max} (m^3/s)	127	17	0.58
pH	2.3 - 3.6	3.0	2.9 - 4.0
Fe_{max} (mg/L)	1390	94	230
Al_{max} (mg/L)	483	63	-
Zn_{max} (mg/L)	145	5.5	70
Cu_{max} (mg/L)	148	3.7	17
Fe_{max} (g/s)	7500	47	69
Al_{max} (g/s)	2700	31	-
Zn_{max} (g/s)	820	2.7	21
Cu_{max} (g/s)	830	1.8	3.7

Table 5. Comparison of flood events in different AMD catchments